ORIGINAL PAPER

A new formulation of the surface charge/surface potential relationship in electrolytes with valence less than three

Oddbjørn Nødland[1] · Aksel Hiorth[1]

Abstract

Surface complexation models (SCMs) based on Gouy-Chapman theory are often used to describe adsorption of ions onto mineral surfaces. To compensate for the buildup of charge at a solid surface, the composition of the electric diffuse layer next to the surface must balance the surface charge. To calculate the diffuse layer composition, several nonlinear equations and integrals must be solved, usually with an iterative approach. Before convergence, charge balance is typically not fulfilled. One numerical difficulty is that, because of these charge balance errors, the iterative solver may attempt to take the square root of a negative number. Herein, we show that for electrolytes containing only monovalent or divalent ions (i.e., most electrolytes encountered in practice), we can greatly simplify the integrals and eliminate the appearance of complex-valued integrands; it is even possible to derive explicit analytical formulas. Furthermore, using the new method prevents converging to non-physical roots of the Grahame equation, which links surface potential to surface charge. To the best of our knowledge, the presented formulation has not been implemented in geochemical modelling software before, although similar mathematical expressions have been presented in the literature. In Gouy-Chapman theory, ions can only be distinguished by their charges, but this is not consistent with all experimental findings. We present a model that allows for the preferential accumulation of ions in the diffuse layer. The model, which is implemented mathematically by including ion exchange sites with a variable exchange capacity, is flexible and more numerically tractable than the standard models for the diffuse layer.

Keywords Geochemical modelling · Surface chemistry · Surface complexation · Diffuse layer · Ion exchange

1 Introduction

Most surface complexation models (SCMs) are based on some variant of Gouy-Chapman theory [1, 2]. In the Gouy-Chapman theory, ions are treated as point charges, and ion concentrations near a charged surface are assumed to follow Boltzmann statistics. From the Poisson equation, one then obtains a mathematical relationship between surface potential and surface charge, the Grahame equation [3–5].

Depending on the problem at hand, one may need to solve the Grahame equation together with a set of other (non-linear) equations, e.g., chemical species mass balance equations. The most common formulation of the Grahame equation has two solutions, only one of which is physical; see equation

(18). To avoid finding the wrong solution, many numerical simulation codes implement a special case instead, for example, by assuming a monovalent electrolyte [6, 7]. However, solving an approximate version of the Grahame equation will generally produce physically inconsistent results.

In addition to respecting the Grahame equation, numerical solvers should correct the mass balance equations to account for accumulation and depletion of ions in the electric diffuse layer next to the charged surface [8]. Borkovec and Westall [9] presented an approach for calculating diffuse layer concentrations. Their suggested method requires the computation of several integrals which may be difficult to resolve numerically, especially when the diffuse layer calculations are needed as a part of solving a larger set of non-linear equations, e.g., during reactive transport simulations. Specifically, when solving the system with an iterative solver such as Newton-Raphson's method, the necessary constraint of charge balance in the bulk solution is not guaranteed to hold until convergence. As a consequence, integrands which are

✉ Aksel Hiorth
aksel.hiorth@uis.no

[1] Department of Energy Resources, University of Stavanger, Stavanger, Norway

not well-defined mathematically may appear during solver iterations.

In this paper we present a simple and robust mathematical approach that works both when we solve the Grahame equation without considering the composition of the counter and co-ions in the diffuse layer, as well as when we do. The idea is to eliminate the total concentration of charge -1 species by assuming charge balance. As long as all charged species are either monovalent or divalent (not a severe limitation, it covers most situations encountered in practice), we can then greatly simplify the surface charge equations. The relevant equations have been implemented in an in-house simulator, IORCoreSim [10, 11], which is capable of both reactive transport and pure equilibrium calculations.

During the writing of this paper, it came to our attention that the same mathematical idea was presented by Oldham [12]. However, the paper by Oldham has mostly been overlooked in the literature. To the best of our knowledge, no other reactive transport simulators have implemented the approach.

The rest of the paper is organized as follows. We start by providing an overview of the geochemical model, including a review of how the Grahame equation can be derived from the Poisson-Boltzmann equation. Next, we present the new method. We illustrate how it improves both solver robustness and numerical accuracy in cases where the Grahame equation is solved without accounting for the diffuse layer composition. Subsequently, the same method is applied to the diffuse layer integration procedure of Borkovec and Westall [9]. Finally, we propose a new model for carbonate minerals that allows for selecting a specific composition of counter ions in the diffuse layer. The model, which is an extension of ion exchange models for cation exchange on clay minerals [6], is capable of describing both anion and cation exchange, depending on the surface charge. We briefly link the model to experimental findings from chalk.

For completeness, we have chosen to include many equations and derivations which are well-known in the literature, but we highlight the novel parts. We also include appendices containing mathematical and numerical details that would disturb the flow of the main text.
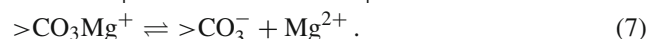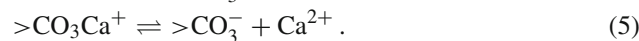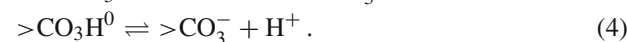
2 Geochemical model

2.1 Aqueous chemistry

To calculate aqueous chemistry, IORCoreSim is based on the standard, textbook approach of dividing the aqueous species into basis and secondary species [13, 14]. Equilibrium constants are computed by the simulator as a function of temperature and pressure from the Helgeson-Kirkham-Flowers (HKF) equation of state [15, 16], coupled with the SUPCRT thermodynamic database [17].

2.2 Surface complexation model for carbonates

Throughout the paper, we will use a SCM developed for calcite surfaces [18, 19]:

$$>CaCO_3^- \rightleftharpoons >CaH_2O^+ + HCO_3^- - H^+ - H_2O. \quad (1)$$
$$>CaOH^0 \rightleftharpoons >CaH_2O^+ - H^+. \quad (2)$$
$$>CaHCO_3^0 \rightleftharpoons >CaH_2O^+ + HCO_3^- - H_2O. \quad (3)$$
$$>CO_3H^0 \rightleftharpoons >CO_3^- + H^+. \quad (4)$$
$$>CO_3Ca^+ \rightleftharpoons >CO_3^- + Ca^{2+}. \quad (5)$$
$$>CaSO_4^- \rightleftharpoons >CaH_2O^+ + SO_4^{2-}. \quad (6)$$
$$>CO_3Mg^+ \rightleftharpoons >CO_3^- + Mg^{2+}. \quad (7)$$

The symbol > is used to distinguish surface complexes from aqueous complexes. In some cases, we will also assume that the solution is in equilibrium with calcite and gaseous CO_2:

$$calcite \rightleftharpoons Ca^{2+} + HCO_3^- - H^+$$
$$CO_2(g) \rightleftharpoons HCO_3^- + H^+ - H_2O. \quad (8)$$
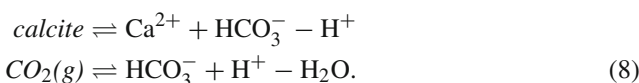
For the above model, we can calculate the surface charge

$$\frac{S_A}{\mathcal{F}}\sigma = [>CaH_2O^+] + [>CO_3Ca^+] + [>CO_3Mg^+]$$
$$- [>CO_3^-] - [>CaCO_3^-] - [>CaSO_4^-], \quad (9)$$

where σ [C/m^2] is the net surface charge density, $\mathcal{F}$=96484.56 C/mol is the Faraday constant, S_A is the specific surface area in units of square meters per litre of water, and the brackets denote molar concentrations of the surface complexes. Each surface complex reaction has a corresponding law of mass action expression; see Table 1 for the log K values used in this study; notice that reactions at the mineral surface are assumed to behave in the same way as the corresponding reactions in the bulk aqueous phase. [19]. Mathematically, the only difference compared to reactions in the aqueous phase is that activities at the surface are corrected to account for electrostatic effects [20]: If the surface is negatively charged, positive ions will have a higher surface activity compared to negative ions, while the opposite is true for a positive surface. As an example, applying the law of mass action to equation (6) yields:

$$\log_{10} K = \log_{10}[>CaH_2O^+] + \log_{10} a_{SO_4^{2-}}$$
$$- \log_{10}[>CaSO_4^-] + 2\underbrace{\frac{\mathcal{F}\psi_0}{\ln 10\, R\, T}}_{\log_{10} E_0}, \quad (10)$$

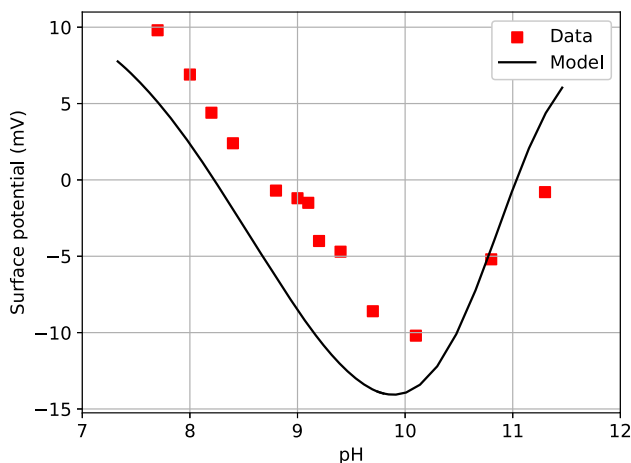For aqueous complexes, the symbol a denotes the thermodynamic activity; herein, computed from Debye-Hückel

theory [21]. We have also introduced E_0 as a shorthand for $\exp(F\psi_0/(RT))$, and more generally we define $E(x) = \exp(F\psi(x)/(RT))$. This is not merely a notational convenience: As we will come back to later, E_0 is used as an additional, "fictive chemical species", to represent the unknown surface potential, $\psi_0 = \psi(0)$. This allows us to write the surface complexation reactions in exactly the same mathematical form as chemical reactions in the aqueous phase.

The carbonate SCM given by Eqs. (1)-(9) is capable of reproducing experimental results; for an example, see Fig. 1. Unless otherwise noted, all simulation results presented in this paper were generated with the carbonate SCM, assuming a specific surface area of 3000 m^2/L, and a site density of 4.95 sites/nm^2 for both calcium ($>CaH_2O^+$) and carbonate ($>CO_3^-$) sites [22]. Irrespective of the choice of model, all simulations presented in this work were conducted at $T = 25°C$.

2.3 Poisson-Boltzmann model for interactions between ions and a charged surface

Except for differences in notation, we follow the development of Borkovec and Westall [9]. The electric potential, ψ[V], is assumed to satisfy the Poisson-Boltzmann equation for a planar surface:

$$\frac{d^2\psi}{dx^2}(x) = -\frac{\mathcal{F}}{\varepsilon\varepsilon_0}\sum_i Z_i \rho_i(x)$$
$$= -\frac{\mathcal{F}}{\varepsilon\varepsilon_0}\sum_i Z_i \rho_i^B \exp\left(-\frac{Z_i\mathcal{F}\psi(x)}{RT}\right), \quad (11)$$

Fig. 1 Comparison between predicted surface potentials from the carbonate SCM and experimentally measured ζ-potentials. The experiments, presented in Fig.4 of [23], were performed at room temperature, using a 5 mM NaCl or $NaHCO_3$ solution. In the simulations, equilibrium with calcite and a fixed partial pressure of CO_2 was assumed [19]
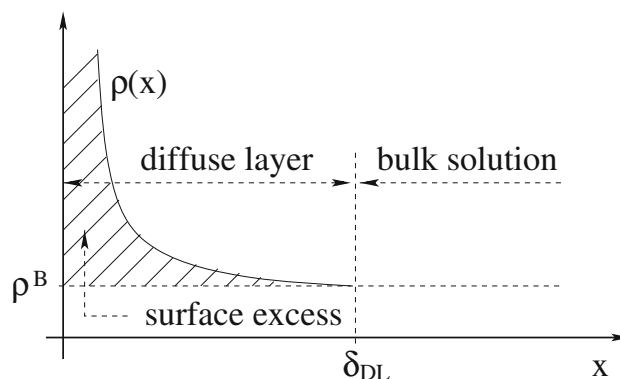
Fig. 2 Ion distribution, $\rho(x)$, near a charged surface

where $\varepsilon_0 = 8.854 \cdot 10^{-12}$ C/V/m is the vacuum permittivity, ε denotes the relative permittivity (dielectric constant) of water, $R = 8.314$ J/K/mol is the ideal gas constant, T is the absolute temperature, $\rho_i(x)$[mol/m^3] is the local concentration of aqueous species i having charge Z_i Fig. 2, and the superscript, B, indicates the bulk concentration far away from the surface ($x \to \infty$). In the second equality, it has been assumed that the local ion concentrations follow Boltzmann statistics.

From Eq. (11), the charge density in the diffuse layer can be calculated by integrating from $x = 0$ (the surface) to infinity, in units of C/m^2:

$$\sigma_{DL} = \mathcal{F}\int_0^\infty \sum_i Z_i \rho_i(x)\, dx$$
$$= -\varepsilon\varepsilon_0 \int_0^\infty dx \frac{d^2\psi}{dx^2} = \varepsilon\varepsilon_0 \left.\frac{d\psi}{dx}\right|_{x=0}. \quad (12)$$

Note that Eq. (11) is non-linear in ψ, which violates the physical principle of superposition. As discussed by Hunter [8], ψ is related to the mean force required to bring an ion from infinity (zero force) close to the charged surface.

2.4 The Grahame equation

It is further assumed that the bulk aqueous solution is charge balanced,

$$\sum_i Z_i \rho_i^B = 0, \quad (13)$$

which implies that both the potential and its derivative vanishes as $x \to \infty$. By differentiating $(d\psi/dx)^2$ according to the chain rule and inserting Eq. (11), the resulting expression can be integrated from infinity to x to yield [9]:

$$\left[\frac{d\psi}{dx}\right]^2 = \frac{2RT}{\varepsilon\varepsilon_0}\sum_i \rho_i^B \left[E(x)^{-Z_i} - 1\right]. \quad (14)$$

By combining Eqs. (12) and (14), we find:

$$\sigma_{DL}{}^2 = 2\,R\,T\,\varepsilon\varepsilon_0 \sum_i \rho_i^B (E_0^{-Z_i} - 1)\,. \qquad (15)$$

By switching to using molar units, $n_i^B = 10^3 \rho_i^B$, we can reformulate the last equation into

$$\sigma_{DL}{}^2 = \kappa_s \cdot \sum_i n_i^B (E_0^{-Z_i} - 1)\,, \qquad (16)$$

where we have defined:

$$\kappa_s \equiv 2 \cdot 10^3 \cdot \varepsilon\,\varepsilon_0\,R\,T\,. \qquad (17)$$

To balance the charge in the diffuse layer with the surface charge, we require $\sigma_{DL} = -\sigma$. By squaring both sides, and inserting (16), we see that one way to ensure this is to solve *the Grahame equation*, $T_{\text{Grahame}} = 0$, where

$$T_{\text{Grahame}} = \kappa_s \cdot \sum_i n_i^B \left(E_0^{-Z_i} - 1 \right) - \sigma^2\,. \qquad (18)$$

Clearly, this equation has two solutions, but only one of them is physical: the solution where the surface charge and surface potential has the same sign. Note that it is possible to avoid two solutions by reformulating Eq. (18) as

$$\begin{aligned} T'_{\text{Grahame}} = {}&\mathrm{sgn}(E_0 - 1)\sqrt{\kappa_s} \\ &\cdot \sqrt{\sum_i n_i^B \left(E_0^{-Z_i} - 1 \right)} - \sigma\,. \end{aligned} \qquad (19)$$

However, this may introduce numerical difficulties as the sum under the square root symbol is only guaranteed to be non-negative when charge balance is fulfilled, and this need not be the case during the non-linear solver iterations. Another reason to prefer Eq. (18) is that the sgn function is discontinuous at $E_0 = 1$.

3 The Grahame equation without computing surface excesses of individual ions

In this section, we compare and contrast several variants of the Grahame equation in the situation where we do *not* correct the mass balance equations for accumulation or depletion of ions in the diffuse layer. In this case a charge imbalance will build up in the solution canceling the surface charge, which is physically incorrect. However, this case is the default option in PHREEQC [24] and it is therefore useful to consider it in some detail. In the next section we will return to the general case.

3.1 New solution method for the mono- or divalent case

The proposed method is valid for an arbitrary combination of monovalent and divalent ions. To derive the necessary equations, we start by introducing a new set of variables, to denote the sum of concentrations of all aqueous species having a given electric charge:

$$n_Z^\Sigma \equiv \sum_{i,\,Z_i = Z} n_i^B\,. \qquad (20)$$

Assuming there are no trivalent ions (ions of valence four or higher are practically non-existent), we can reformulate the Grahame equation by replacing the individual ion concentrations with n_1^Σ, n_{-1}^Σ, n_2^Σ, and n_{-2}^Σ. For species having charges +1, +2, or -2, Eq. (20) is applied directly, by inserting concentrations proposed by the numerical simulator on the right-hand side. On the other hand, the total concentration of charge -1 species is *calculated*, by assuming charge balance:

$$n_{-1}^\Sigma = n_1^\Sigma + 2(n_2^\Sigma - n_{-2}^\Sigma)\,. \qquad (21)$$

In other words, the concentrations of OH$^-$, Cl$^-$, etc. are ignored for the purpose of solving the Grahame equation: Instead, n_{-1}^Σ is eliminated from Eq. (18) by inserting Eq. (21). After some algebra, we end up with an expression having only the physical root:

$$T_{\text{Grahame}}^{\pm 1, \pm 2} = 2\sqrt{\kappa_s \mathcal{I}_d} \sinh\left(\frac{\mathcal{F}\psi_0}{2RT} \right) - \sigma\,. \qquad (22)$$

Here, we have defined:

$$\mathcal{I}_d \equiv n_1^\Sigma + n_2^\Sigma \left(2 + \frac{1}{E_0}\right) + n_{-2}^\Sigma E_0\,. \qquad (23)$$

3.1.1 Recovering the special case of a symmetrical electrolyte

Let $\mathcal{I}$ denote the ionic strength of the solution in molar units. After eliminating n_{-1}^Σ by enforcing charge balance, we get

$$\mathcal{I} = n_1^\Sigma + 3n_2^\Sigma + n_{-2}^\Sigma\,, \qquad (24)$$

for a general mix of mono- and divalent ions. For a symmetrical electrolyte of valence Z, electroneutrality implies that

$$\mathcal{I} = Z^2 n_Z^\Sigma = Z^2 n_{-Z}^\Sigma\,. \qquad (25)$$

Thus, we immediately deduce that for a monovalent electrolyte, $\mathcal{I}_d = \mathcal{I}$. Similarly, for a divalent electrolyte:

$$\mathcal{I}_d = \frac{\mathcal{I}}{4} \frac{(E_0 + 1)^2}{E_0} = \mathcal{I} \cosh^2 \left(\frac{\mathcal{F}\psi_0}{2RT} \right) \ . \tag{26}$$

In both cases, Eq. (22) reduces to

$$\sigma = -\sigma^{DL} = 2 \frac{\sqrt{\kappa_s \mathcal{I}}}{Z} \cdot \sinh \left(\frac{Z\mathcal{F}\psi_0}{2RT} \right) , \tag{27}$$

where we have used the trigonometric identity $\cosh(x/2)\sinh(x/2) = \sinh(x)/2$.

Equation (27) can also be derived directly from Eq. (18), by noting that

$$\sum_i n_i^B (E^{-Z_i} - 1) = \frac{I}{Z^2} \left(E^Z + E^{-Z} - 2 \right)$$
$$= 4 \frac{I}{Z^2} \sinh^2 \left(\frac{Z\mathcal{F}\psi}{2RT} \right) . \tag{28}$$

Thus, Eq. (27) is valid for the (theoretical) case $Z \geq 3$ as well.

3.1.2 The Grahame equation in other numerical simulators

In the numerical simulation literature, Eq. (27) with $Z = 1$ is frequently referred to as *the Gouy-Chapman equation* [6, 7]. This formula is sometimes used regardless of the ionic composition, presumably to avoid the appearance of unphysical roots.

Some authors also report using a variant of Eq. (27), in which $Z > 1$ appears in the argument to the hyperbolic sine, but $Z = 1$ in the constant prefactor outside [7, 25]. For the divalent case, this leads to an extra factor 2 in front of the hyperbolic term, compared to the "true solution". On the other hand, if the equation is rewritten in terms of the total concentration of cations / anions, rather than ionic strength, the constant prefactor becomes the same for all values of Z [6, 26].

3.2 Example: Unphysical solutions (sea water + calcite)

As a first example, we considered the equilibration of sea water with calcite. Regardless of whether we solved Eq. (27) with $Z = 1$, Eq. (27) with $Z = 2$, or Eq. (22), the predicted surface charge and surface potential was the same in all cases, almost zero but slightly negative ($\psi_0 = -0.7$ mV, $\sigma = -0.001$ C/m^2). We remark that experimentally reported ζ-potentials for the calcite-sea water interface have been reported as slightly more negative, though results vary [27–29].

On the other hand, the calculated surface charge had the opposite sign as the surface potential when Eq. (18) was used, an unphysical result. For a visual illustration of the same fact, we implemented a variant of the geochemical solver in which the Grahame equation was solved as a 1D problem; that is, it was handled separately from all the other equations in the system by fixing the value of ψ_0 during Newton iterations. Figure 3 clearly demonstrates that when solving Eq. (18), the numerical solution will be sensitive to the initial guess. This problem is avoided when using Eq. (22), as illustrated by the red, straight line in the figure.

3.3 The Grahame equation at low values of the surface potential

In the previous example, we got virtually identical values for σ and ψ_0, independent of whether we assumed a monovalent electrolyte, a divalent electrolyte, or a mixed electrolyte. This was due to $|\psi_0|$ being small: Indeed, a quick comparison of Eqs. (23) and (24) reveals that in the limit $\psi_0 \to 0$ ($E_0 \to 1$, hence also $\sigma \to 0$):

$$\mathcal{I}_d \to n_1^\Sigma + 3n_2^\Sigma + n_{-2}^\Sigma = \mathcal{I} ,$$

proving that (22) becomes the same as Eq. (27) with $Z = 1$. Similarly, we can linearize the hyperbolic sine term in the formula for symmetrical electrolytes,

$$\sinh \left(\frac{Z\mathcal{F}\psi_0}{2RT} \right) \approx \frac{Z\mathcal{F}\psi_0}{2RT} . \tag{29}$$
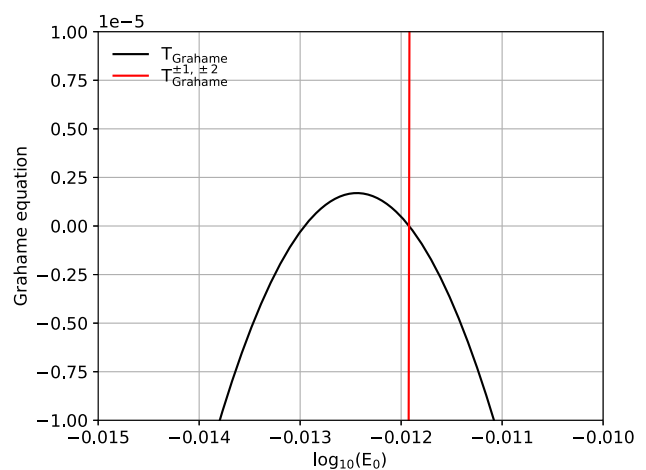
Fig. 3 Equilibration of sea water with calcite: Example calculations in which ψ_0 was kept fixed when solving the multidimensional system of chemical equations. The figure was generated by systematically varying the value of ψ_0. For each value of ψ_0, the other equations were solved, after which the Grahame equation was evaluated. Note that the logarithm of E_0 is plotted on the x-axis, rather than ψ_0, because this is the unknown used by the simulator. Black, solid line: Using equation (18). Red, solid line: Using equation (22)

As expected, the expressions for the divalent and monovalent cases agree at low surface potentials (the Z-terms cancel).

3.4 Example: Fixed surface charge

To study the behavior of the Grahame equation in isolation, we temporarily abandoned the carbonate SCM, and considered a much simpler model without any mineral dissolution / precipitation or surface complexation, hence the surface charge was constant. Chemical reactions in the aqueous phase were also largely or fully ignored.

To focus on the different behavior of monovalent versus divalent ions, we replaced the sea water brine with a much simpler 2:1-electrolyte, Na_2SO_4. Figure 4 shows calculated spatial profiles of the potential, when a surface with charge $\pm 0.05\,C/m^2$ was placed into contact with a 24 mM Na_2SO_4 solution. It is clear from the figure that using an approximate version of the Grahame equation leads to incorrect results. The error of assuming a symmetrical electrolyte depends on the sign of the surface charge. For a negatively charged surface, the counter ions that accumulates near the surface are Na^+ ions, hence the formulas valid for monovalent electrolytes provide a decent approximation. On the other hand, when $\sigma > 0$ it is mainly SO_4^{2-} ions that have a high surface concentration, thus it is better to use the divalent electrolyte approximation.

To summarize, for a brine with only mono- and/or divalent ions:

- The specialization of the Grahame equation to symmetrical electrolytes, Eq. (27), is only valid at low surface potentials.
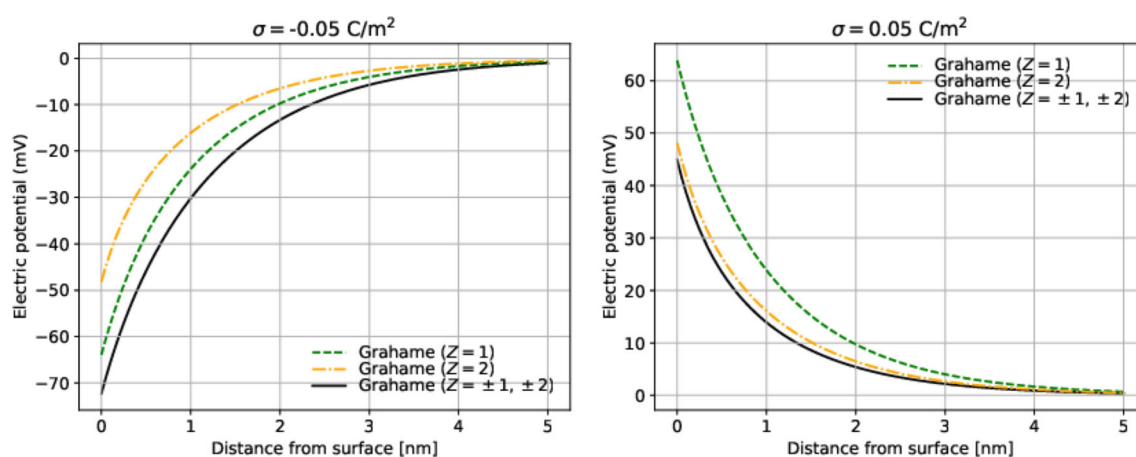
- If one insists on using Eq. (27) at higher potentials, the error will be reduced by choosing Z to be the valence of the dominating counter ion(s). However, it may be difficult to implement code logic to do this consistently, especially for large, complex reactive transport simulations.
- Equation (27) should generally not be used to calculate the composition of the diffuse layer.
- Using Eq. (22) avoids having to consider this source of numerical error, and is therefore recommended.

4 Diffuse layer model with surface excess calculations

So far, we have not corrected the mass balance equations to account for accumulation and depletion of ions in the diffuse layer. These corrections are usually very small, but there are situations where they matter, e.g., in certain reactive transport simulations where we have to ensure that the bulk solution of each grid block is electrically neutral following transport calculations (see Fig. 5). Especially in simulations with many grid blocks, small charge imbalances sometimes accumulate to create a noticeable impact on, e.g., predicted pH.

For carbonates, the effect of diffuse layers could be significant. For example, in one set of coreflooding experiments it was found that by adding sulfate to the injection brine, the effective cation exchange capacity of chalks could be increased by a factor of two [30, 32]. The interpretation was that adsorption of sulfate created a negative surface charge, due to the reaction in Eq. (6), and as a consequence, more cations were removed from the flowing solution. These studies, as well as many others in the literature, have furthermore

Fig. 4 Spatial profiles of the potential for a 24 mM Na_2SO_4 brine, assuming a constant surface charge. Only the value of ψ_0 was calculated by the numerical simulator; $\psi(x)$ for $x > 0$ was computed based on ψ_0 in a separate script. The aqueous complexes $NaSO_4^-$, $NaOH^0$, and HSO_4^- were removed from the HKF geochemical database before conducting any simulations. Left: $\sigma = -0.05\,C/m^2$. Right: $\sigma = +0.05\,C/m^2$
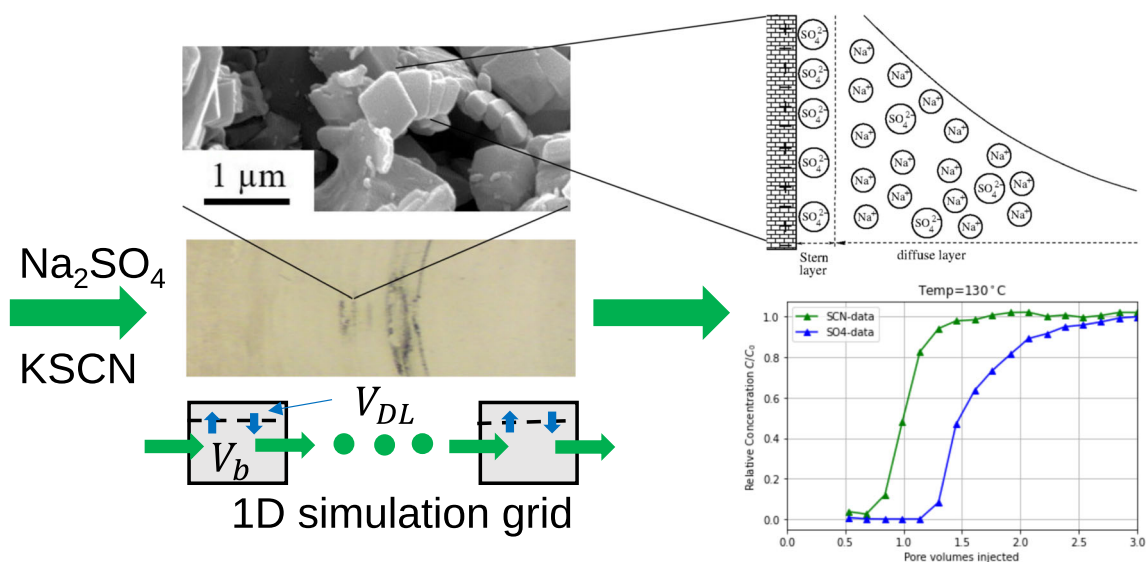
Fig. 5 Experimental results when a Na$_2$SO$_4$ solution flooded through a chalk core [30], SEM image adopted from [31]. (Top) Conceptual picture of the ion distribution near a negatively charged surface. (Bottom) An illustration of one method to maintain charge balance during numerical transport calculations (here, only advection): First, flowing concentrations are updated by treating the ions in the diffuse layer as immobile. Next, ions are redistributed between the solution and the surface. The size of the diffuse layer has been exaggerated for visualization purposes

stressed the importance of ion-specific effects, but the Gouy-Chapman theory is only able to distinguish between ions in the diffuse layer based on their charges. It has been suggested that the affinity of a cation for the mineral surface also depends on the size of the cation. For clay minerals in particular, it has been observed that when two cations have the same charge, the one with the larger *non-hydrated* radius tends to be preferred [33]. This trend is opposite to what one would expect from a naive application of Coulomb's law, according to which the electrostatic attraction between a cation and the surface should decrease with increasing ionic radius.

A typical resolution of this seeming paradox is that larger cations attract fewer water molecules, hence these ions have a smaller *hydrated* radius and can therefore come closer to the mineral surface [33]. All else being equal, K$^+$ should therefore be more strongly retained than Na$^+$, and Ca^{2+} more so than Mg^{2+} [34]. Consistent findings have not always been found, however, e.g., the degree of cation selectivity seems to depend on the clay mineral type [35, 36]. Moreover, ions of similar hydrated radius have been observed to behave differently, e.g., Cs$^+$ and Rb$^+$ [37]. To explain such data, mineral heterogeneity has sometimes been invoked [38]. It has also been pointed out that since weakly hydrated cations are easily dehydrated, they can adsorb more strongly than cations with larger solvation shells [39, 40].

Regardless of the fundamental explanation, it makes sense to develop a model for carbonates that allows for a selective uptake in the diffuse layer. To this end, we will present an ion

exchange model for carbonates where it is possible to distinguish between ions of the same charge in the diffuse layer. However, we will first present the general mass conservation equations used, and discuss how Gouy-Chapman theory, as described by Borkovec and Westall [9], allows us to calculate the diffuse layer composition when ions of the same charge are treated equally.

4.1 Mass conservation in the presence of a diffuse layer

The diffuse layer contains both negative and positive ions, as illustrated in Fig. 5. The number of moles of an arbitrary ion i in the diffuse layer is (see Fig. 2)

$$N_{\mathrm{DL},i} = A \int_0^{\delta_{\mathrm{DL}}} \rho_i(x)\mathrm{d}x , \tag{30}$$

where A [m^2] is the pore surface area, and δ_{DL} [m] is the size of the diffuse layer (for simplicity, assumed constant). We can expand this as:

$$N_{\mathrm{DL},i} = A \int_0^{\delta_{\mathrm{DL}}} (\rho_i(x) - \rho_i^B)\mathrm{d}x + A \int_0^{\delta_{\mathrm{DL}}} \rho_i^B \mathrm{d}x,$$
$$= A \int_0^{\delta_{\mathrm{DL}}} (\rho_i(x) - \rho_i^B)\mathrm{d}x + A\delta_{\mathrm{DL}}\rho_i^B . \tag{31}$$

At the edge of the diffuse layer $\rho_i(x) \simeq \rho_i^B$, thus we replace the upper integration limit by ∞[1]. After also changing units from $m^3 \rightarrow L$, we find:

$$N_{\text{DL},i} \simeq V_w g_{Z_i} n_i^B + V_{\text{DL}} n_i^B = V_w n_i^B (g_{Z_i} + f_{\text{DL}}), \quad (32)$$

where V_w [L] is the total volume of water in the pore, $f_{\text{DL}} = V_{\text{DL}}/V_w$ is the volume fraction occupied by the diffuse layer, and the dimensionless factor g_{Z_i} is:

$$
\begin{aligned}
g_{Z_i} &= \frac{10^3 \cdot S_A}{n_i^B} \int_0^\infty \left(n_i(x) - n_i^B \right) dx \\
&= \frac{10^3 \cdot S_A}{n_i^B} \int_0^\infty n_i^B \left(E(x)^{-Z_i} - 1 \right) dx.
\end{aligned}
\quad (33)
$$

Let N_i denote the total number of moles of ion i. In addition to the diffuse layer part, the total includes the number of moles in the bulk solution, $N_{B,i} = V_B n_i^B$ where V_B [L] $= V_w - V_{\text{DL}}$ is the volume of the bulk aqueous phase, as well as the number of moles adsorbed at the surface in the form of either a surface complex or an ion exchange complex:

$$
\begin{aligned}
N_i &= V_w g_{Z_i} n_i^B + V_{\text{DL}} n_i^B + V_B n_i^B + V_w (n_i^S + n_i^{IE}) \\
&= V_w \left(g_{Z_i} n_i^B + n_i^B + n_i^S + n_i^{IE} \right),
\end{aligned}
\quad (34)
$$

where the surface concentrations n_i^S and n_i^{IE} are given in units of molarity.

By dividing by V_w, we can reformulate the mass conservation equation in terms of concentrations rather than moles:

$$n_i^{\text{Tot}} \equiv \frac{N_i}{V_w} = n_i^B (1 + g_{Z_i}) + n_i^S + n_i^{IE}. \quad (35)$$

4.2 Mass balances in terms of basis and secondary species

For completeness, we explain how the system of chemical species mass balance[2] equations is formulated in IOR-CoreSim. The simulator uses the approach described by [14, 17], wherein the set of geochemical species are partitioned into two subsets: basis species and secondary species. The choice of basis species is not unique, but for a given choice of basis, concentrations of secondary species can be expressed uniquely as functions of the basis species concentrations. As a result, only the basis species concentrations are treated as unknowns when solving the system.

As mentioned previously, surface complexes are treated mathematically in the same way as aqueous complexes, which is possible by adding the fictive species E_0 to the list of basis species. Some of the surface complexes are also included in the basis set.

In the rest of this subsection, we employ a slightly different notation than in the rest of the paper. Let m_i denote the molar concentration an arbitrary basis specie, relative to the total water volume, and let n_i be the concentration of an arbitrary secondary specie. Let m_i^{Tot} be the total concentration corresponding to basis specie i, that is, the sum of m_i and the concentrations of all secondary species that react with basis specie i in an equilibrium reaction. According to Eq. (35), we then have

$$m_i^{\text{Tot}} = (1 + g_{Z_i})m_i + \sum \mu_{ji}(1 + g_{Z_j})n_j^{\text{aq,scomp}}, \quad (36)$$

where μ_{ji} is the stoichiometric matrix which describes how secondary species are formed from basis species. The superscript has been added to emphasize that secondary species include both aqueous and surface species, with the understanding that the g_{Z_i}-terms are zero for surface species. From Eq. (32), we see that the contribution to (36) from the diffuse layer is:

$$
\begin{aligned}
m_{DL,i}^{\text{Tot}} &\equiv \frac{N_{\text{DL},i} + \sum \mu_{ji} N_{\text{DL},j}}{V_w} \\
&= (f_{\text{DL}} + g_{Z_i})m_i + \sum \mu_{ji}(f_{\text{DL}} + g_{Z_i})n_j^{\text{aq}}.
\end{aligned}
\quad (37)
$$

Note that g_{Z_i} may be negative and it is important that f_{DL} is not too small to avoid negative concentrations in the diffuse layer.

For even more details on how we solve the carbonate SCM, see the example in Section 4.6.

4.3 Reformulating the relationship between σ and ψ_0

In the rest of the paper, we shall once again ignore the distinction between basis and secondary species. To calculate the accumulation / depletion of charged species in the diffuse layer, we follow the development of Borkovec and Westall [9] and introduce the *surface excess* of an ion in the diffuse layer, in units of moles per litre:

$$n_i^\Gamma \equiv 10^3 \cdot S_A \int_0^\infty \left(n_i(x) - n_i^B \right) dx. \quad (38)$$

By definition, the previously introduced g_{Z_i}-factor is the ratio between the surface excess and bulk concentration:

$$n_i^\Gamma = g_{Z_i} \cdot n_i^B. \quad (39)$$

---

[1] This is equivalent to assuming that $\psi(\delta_{\text{DL}}) = 0$. Alternatively, we could keep the integration limit, but then the value of the surface potential should be known at the edge of the diffuse layer.

[2] Strictly speaking by "mass balance" we mean conservation of chemical elements, but it is common in the geochemical literature to use the term mass balance.

Equation (12) can be used to derive an alternative expression for the diffuse layer charge density:

$$\sigma_{DL} = \frac{\mathcal{F}}{S_A} \sum_i Z_i n_i^{\Gamma} = \frac{\mathcal{F}}{S_A} \sum_i Z_i g_{Z_i} n_i^B, \qquad (40)$$

where once again charge-balance of the bulk solution has been invoked, $\sum Z_i n_i^B = 0$. Thus, instead of solving Eq. (22) or any of its symmetrical variants, we can solve $T_\sigma^{DL} = 0$, where

$$T_\sigma^{DL} = \frac{S_A}{\mathcal{F}} (\sigma_{DL} + \sigma)$$
$$= \sum_i Z_i g_i n_i^B + \sum_i Z_{sci} n_i^S. \qquad (41)$$

Given that diffuse layer concentrations are calculated and included in the mass balance, and that the bulk solution is electrically neutral, a solution to $T_\sigma^{DL} = 0$ should automatically satisfy Eq. (18) as well. An advantage of using Eq. (41) is that we explicitly enforce the charge balance between the surface and the diffuse layer with one equation.

As a side note, we remark that when run in default mode, the popular simulation program PHREEQC *does not* compute the composition of the diffuse layer. Instead, the monovalent approximation to the Grahame equation is used, Eq. (27) with $Z = 1$ [24]. As we have seen, this will produce physically inconsistent results for arbitrary brines. On the other hand, if the *diffuse_layer*-flag is added to the input file, PHREEQC attempts to use the integration procedure of [9], in which case an equation akin to (41) is solved. At convergence, the solution should also satisfy Eq. (18), however Eq. (18) is not implemented directly, as has been suggested [7].

4.4 Calculating surface excesses in the diffuse layer

A formula for the dimensionless g_Z-factors can be derived from Eq. (14) by performing the variable substitution $x \rightarrow E$:

$$g_Z = \frac{S_A \sqrt{\kappa_s}}{2\mathcal{F}} \qquad (42)$$
$$\cdot \int_1^{E_0} \frac{\left(E^{-Z} - 1\right) dE}{\text{sgn}(E_0 - 1) \left[E^2 \sum_j n_j^B (E^{-Z_j} - 1)\right]^{1/2}}.$$

Except in special cases (see Appendix A), the integrals (42) must be computed numerically. A practical challenge is that the integrands may not always have physically meaningful values. This is because there is no guarantee that the bulk solution will be electrically neutral until *after* convergence. During the non-linear solver iterations, if the charge balance error is sufficiently large, the term under the square root in

the denominator can become negative [9]. Unless explicitly handled, this will cause the solver to crash.

4.5 New method for calculating diffuse layer concentrations

As with Eq. (18), we can greatly simplify the integrals if we assume that 1) there are only ± 1 and ± 2 charges, and 2) charge-balance is satisfied. First, if we use Eq. (21) to eliminate n_{-1}^{Σ} from the denominator, we get:

$$E^2 \sum_j n_j^B (E^{-Z_j} - 1) = E(E - 1)^2 \mathcal{I}_d. \qquad (43)$$

The integrals (42) then become:

$$g_Z = \frac{S_A \sqrt{\kappa_s}}{2\mathcal{F}} \int_1^{E_0} \frac{E^{-Z} - 1}{(E - 1)\sqrt{E \mathcal{I}_d}} dE. \qquad (44)$$

After inserting (23), we find:

$$g_1 = -\frac{S_A \sqrt{\kappa_s}}{2\mathcal{F}} \int_1^{E_0} \frac{E^{-3/2}}{\mathcal{I}_d^{1/2}} dE. \qquad (45)$$

$$g_2 = -\frac{S_A \sqrt{\kappa_s}}{2\mathcal{F}} \int_1^{E_0} \frac{E^{-5/2}(E + 1)}{\mathcal{I}_d^{1/2}} dE. \qquad (46)$$

$$g_{-1} = \frac{S_A \sqrt{\kappa_s}}{2\mathcal{F}} \int_1^{E_0} \frac{E^{-1/2}}{\mathcal{I}_d^{1/2}} dE. \qquad (47)$$

$$g_{-2} = \frac{S_A \sqrt{\kappa_s}}{2\mathcal{F}} \int_1^{E_0} \frac{E^{-1/2}(E + 1)}{\mathcal{I}_d^{1/2}} dE. \qquad (48)$$

Since $\mathcal{I}_d > 0$ (there are always some H^+ ions), the integrands will never take on complex values, hence all four integrals are easily evaluated.

4.6 Example: 0.024 M Na₂SO₄ brine in equilibrium with calcite and CO₂

In the example, seven aqueous basis species are used: Ca^{2+}, Cl^-, H^+, H_2O, HCO_3^-, Na^+, and SO_4^{2-}. Including surface chemistry introduces three more basis species: $>CaH_2O^+$, $>CO_3^-$, and E_0, the latter representing surface charge. The secondary species are listed in Table 1, along with the equilibrium reactions for how they dissociate into basis species.

In principle, we therefore need ten independent equations to determine the equilibrium chemistry. However, the activity of water is assumed to be unity, thus water need not be included as an unknown. Further simplifications can be made by considering the law of mass action equations for calcite and CO₂ equilibria, i.e., the last two equations in Table 1. Solving these equations allows us to express the calcium and

bicarbonate activities as a function of the H^+ activity, effectively removing Ca^{2+}, and HCO_3^- as independent variables and further reducing the number of unknowns to seven. A more general treatment of how to handle mineral equilibria is to use the basis swapping method described in [14].

Next, there are four mass balance equations for Na^+, SO_4^{2-}, $>CaH_2O^+$, and $>CO_3^-$, see Eq. (36). To solve for H^+, we include an equation for the charge balance of the solution, Eq. (13). Finally, there is one equation for the charge balance between the diffuse layer and the surface, Eq. (41), and one equation to determine the surface charge, Eq. (9).

When the Newton-Raphson iterations start, the activities of $>CaH_2O^+$, $>CO_3^-$, Na^+, and SO_4^{2-} are set equal to the corresponding total concentrations. The initial guess for the surface potential and charge are zero, and the activity of H^+ is set equal to neutral pH. The ionic strength and activity coefficients are updated in-between of each Newton-Raphson iteration, i.e., we follow the "soft formulation" described in [14]. The numerical integrals are calculated using a 10 point Gauss-Legendre quadrature. We also tried to implement the analytical results described in Appendix A, but found that it was faster to estimate the surface excess integrals using numerical integration of Eq. (45)-(48).

The input total concentrations and computed final concentrations are listed in Table 3. The estimated concentration of H^+ in the water phase is negative, but this is an artifact due to the fact that we have not accounted for the concentration of water (which contains a lot of hydrogen). Observe also that the surface excess for sodium is positive, while it is negative for sulfate.

In the cases we have considered so far, the calculations converged fast. Typically, only 5-10 Newton-Raphson iterations were required to reach the desired accuracy.

5 Alternative ion exchange model for carbonate rocks

From Eq. (33) it is clear that the diffuse layer model does not treat ions individually; all that distinguishes two ions is their charges and concentrations. We would also like to test models with a selective uptake of ions in the diffuse layer, e.g. exclude tracer molecules from the diffuse layer. There are also indications from core floods that some ions are preferred, e.g. K^+ over Ca^{2+}[30, 32]. However, the exact reason for this observation requires in-depth analysis that is beyond the scope of this paper.

We want a model that...

1. ...conserves charge in the diffuse layer, and
2. ...can account for the preferential adsorption of divalent ions over monovalent ions, yet

3. ...is also capable of selecting certain ions of the same charge over others; e.g., excluding tracers from the diffuse layer.

As an alternative model for carbonate rocks, we suggest introducing a set of ion exchange reactions. This is often done to model adsorption onto clay minerals, however for clays it is usually assumed that the rock has a fixed negative exchange capacity which stems from charge imbalances in the crystal structure. In contrast, we want to allow for both positive and negative ions in the diffuse layer, hence we need positive and negative exchange sites.

Let Y_{DL}^- denote the total exchange capacity for positive ions in the diffuse layer, in units of equivalents per litre or water. Similarly, let Y_{DL}^+ be the total exchange capacity for negative ions. Each exchanger ($Y_{DL}^\pm$) has opposite sign as the ions it attracts, hence:
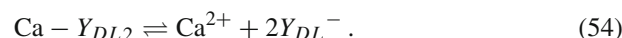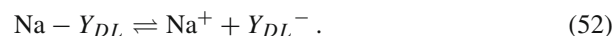
$$Y_{DL}^- \equiv \sum_{Z_i > 0} Z_i n_i^B \left[g_{Z_i} + f_{DL} \right], \tag{49}$$

$$Y_{DL}^+ \equiv - \sum_{Z_i < 0} Z_i n_i^B \left[g_{Z_i} + f_{DL} \right]. \tag{50}$$

Because of the valence terms in the above expressions, divalent ions will occupy two sites on the exchangers. The net charge of the ion exchangers has to balance the net charge in the diffuse layer:

$$\begin{aligned} Y_{DL}^- - Y_{DL}^+ &= \sum_i Z_i n_i^B \left[g_{Z_i} + f_{DL} \right] \\ &= \sum_i Z_i g_{Z_i} n_i^B \\ &= \frac{S_A}{\mathcal{F}} \sigma_{DL}. \end{aligned} \tag{51}$$

Next, we want to reshuffle ions, e.g., exchange calcium for sodium in the diffuse layer, or exclude certain ions. Mathematically, we define half-reactions [41] for all ions of interest:

$$Na - Y_{DL} \rightleftharpoons Na^+ + Y_{DL}^-. \tag{52}$$
$$H - Y_{DL} \rightleftharpoons H^+ + Y_{DL}^-. \tag{53}$$
$$Ca - Y_{DL2} \rightleftharpoons Ca^{2+} + 2Y_{DL}^-. \tag{54}$$
$$HCO_3 - Y_{DL} \rightleftharpoons HCO_3^- + Y_{DL}^+ \tag{55}$$
$$SO_4 - Y_{DL2} \rightleftharpoons SO_4^{2-} + 2Y_{DL}^+. \tag{56}$$

More generally, for any ion i:

$$i - Y_{DL|Z_i|} \rightleftharpoons i^{Z_i} + |Z_i| Y_{DL}^{-\mathrm{sign}(Z_i)}. \tag{57}$$

When applying the law of mass action to Eq. (57), we define the activity of an ion exchange complex according to the Gaines-Thomas convention [6, 42].

By manipulating the $\log K$ values for the exchange reactions, we can alter the distribution of ions in the diffuse layer. The $\log K$ values must be determined from experiments. However, in this paper we will only illustrate the behaviour of the model by picking a few hypothetical scenarios.

5.1 Simplification: Only counter ions

The ion exchange reactions are easily implemented by adding $Y_{DL}{}^{\pm}$ to the list of basis species, and by treating the exchange species as secondary species. The difficult part is how to calculate the variable exchange capacity. This is because the total number of exchange sites in Eqs. (49) and (50) depend on the complicated g_{Z_i}-factors. To avoid having to evaluate these factors, we make the simplifying assumption that it is only the counter ions that balance the surface charge, i.e., ions with the opposite charge as the surface. Then, the exchange capacity of the counter ions can be related directly to the surface charge, via Eq. (22). For simplicity, we shall assume that the surface charge is negative (the case with $\sigma > 0$ is entirely similar), in which case:

$$
\begin{aligned}
Y_{DL}{}^{-} &= -\frac{S_A}{\mathcal{F}}\sigma + f_{DL}\sum_{Z_i=1,2} Z_i n_i \\
&= -\frac{2S_A}{\mathcal{F}}\sqrt{\kappa_s \mathcal{I}_d}\sinh\left(\frac{\mathcal{F}\psi_0}{2RT}\right) \\
&\quad + f_{DL}\sum_{Z_i=1,2} Z_i n_i \, .
\end{aligned}
\tag{58}
$$

$$
Y_{DL}{}^{+} = -f_{DL}\sum_{Z_i=-1,-2} Z_i n_i \, .
\tag{59}
$$

From these expressions, it is possible to calculate the composition of the diffuse layer without calculating any time-consuming integrals. Note that (51) still holds. The algorithm is as follows:

1. Define additional basis species $Y_{DL}{}^{\pm}$ with corresponding half-reactions, e.g., Eqs. (52)-(56).
2. Set $\psi = 0$, and compute the total concentration of the exchange species from Eq. (59).
3. Solve Eq. (36) for each basis specie (including the exchange species $Y_{DL}{}^{\pm}$) together with Eq. (22) to obtain preliminary activities and concentrations of all basis species, hence also ψ and σ. When equilibrium phases are included in the calculation, we use the basis-swapping technique described by Bethke [14].
4. Use the estimated values of ψ and σ to update the exchange capacities, then go to 3.

It would be possible to solve all equations inside each Newton-Raphson iteration, but so far we have found that simply updating the exchanger concentrations in an external loop works well. Such a loop is used anyway by the solver, to update activity coefficients and the ionic strength.

5.2 Ion exchange model: 0.024 M Na$_2$SO$_4$ brine in equilibrium with calcite and CO$_2$

As before, when calcite and CO$_2$ is used as equilibrium phases, the Ca^{2+} and HCO$_3^{-}$ concentrations are determined from the equilibrium reactions, and the pH is determined by requiring charge balance. The computed solution chemistry is shown in Table 4; observe that $Y_{DL}{}^{-} - Y_{DL}{}^{+} = \frac{S_A}{\mathcal{F}}\sigma$, as should be the case.

By modifying the $\log K$ values for the half-reactions, we obtain a selective uptake of ions on the exchanger: Table 5 lists some example cases. The calculated diffuse layer

Fig. 6 Composition of the diffuse layer obtained with five different models. Left: Diffuse layer model with calculation of surface excess. Column 2-5: ion exchange model with $\log K$ values as listed in Table 5
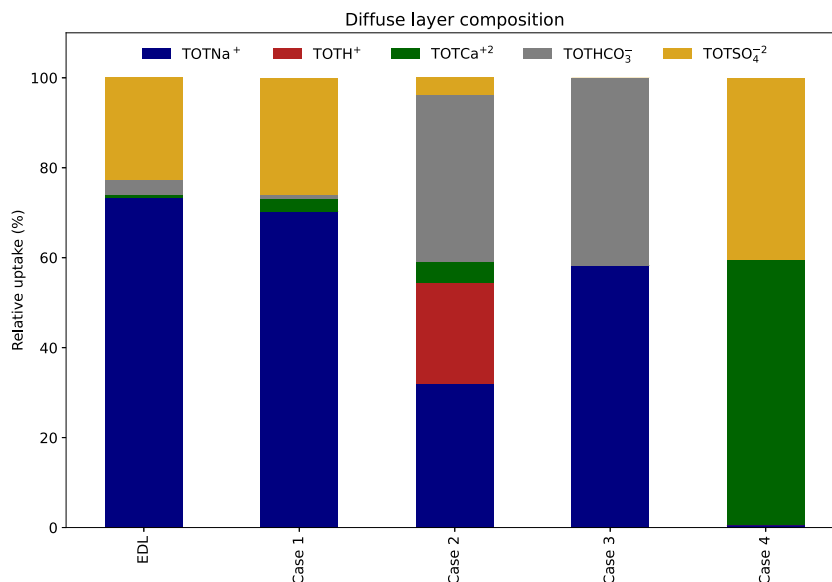
concentrations are presented in Table 6 and plotted in Fig. 6 as percentages of the total. Observe that for the case where all $\log K$ values are equal (case 1), the results are quite similar as for the previous model without the exchange reactions.

6 Conclusion

There are at least two numerical challenges when implementing SCMs: (i) the Grahame equation, Eq. (18), has two solutions of which only one is physically relevant, and (ii) the numerical method for calculating concentrations in the diffuse layer can fail, due to the appearance of integrands with complex values during Newton-Raphson iterations. We have presented a solution approach which circumvents both problems. Our method is valid for the case when all ions are either mono- or divalent. Usually, this is not a severe restriction, because concentration of ions with valence three or higher tend to be very low.

We have also investigated the impact of replacing the Grahame equation with a special case valid for symmetrical electrolytes. We have demonstrated that the surface potential obtained from such a model should not be used to calculate the diffuse layer composition, because the charge in the diffuse layer will not be correctly balanced by the surface charge.

Regardless of which model is used to calculate surface charge, the conventional Poisson-Boltzmann equation treats ions of the same valence equally: It is not possible to describe selective adsorption of ions in the diffuse layer. However, this may be needed to describe experimental results, e.g., from carbonates. As an alternative, we have presented a model in which the diffuse layer is treated like an ion exchanger with a variable number of exchange sites. The model has yet to be tested against experimental data, which is needed to determine reasonable $\log K$ values.

Appendix A Analytical calculation of diffuse layer integrals

When there are only ± 1 and ± 2 species, it is possible to find explicit formulas for the diffuse layer concentrations. By substituting $\nu \equiv 1 - 1/E$, Eq. (42) becomes

$$g_Z = \frac{S_A}{2\mathcal{F}} \sqrt{\frac{\kappa_s}{\mathcal{I}}} \int_0^{\nu_0} \frac{(1-\nu)^Z - 1}{\nu\sqrt{q\nu^2 - p\nu + 1}} \, d\nu, \tag{A1}$$

for $\nu_0 = 1 - 1/E_0 = (E_0 - 1)/E_0$, and where:

$$p \equiv \frac{n_1^\Sigma + 4n_2^\Sigma}{\mathcal{I}}. \tag{A2}$$

$$q \equiv \frac{n_2^\Sigma}{\mathcal{I}}. \tag{A3}$$

The ionic strength is given by Eq. (24). Note that we always have $\nu < 1$, because $\nu = 1$ would imply an infinite surface potential.

Symmetrical electrolyte

For a symmetrical electrolyte of valence Z, it is straightforward to show [9]:

$$g_{\pm Z} = \frac{S_A}{\mathcal{F}} \sqrt{\frac{\kappa_s}{\mathcal{I}}} \left[(1 - \nu_0)^{\pm Z} - 1 \right]. \tag{A4}$$

Mix of mono- and divalent ions

When all charge types are present, surface excesses of monovalent ions can be computed from [12]:

$$g_1 = \frac{S_A}{\mathcal{F}} \sqrt{\frac{\kappa_s}{\mathcal{I}}} \frac{1}{2\sqrt{q}} \left[\cosh^{-1}\left(\frac{p - 2q\nu}{\sqrt{p^2 - 4q}} \right) \right]_0^{\nu_0}. \tag{A5}$$

$$g_{-1} = \frac{S_A}{\mathcal{F}} \sqrt{\frac{\kappa_s}{\mathcal{I}}} \frac{1}{2\sqrt{q - p + 1}} \\ \cdot \left[\cosh^{-1}\left(\frac{2 - p - \nu(p - 2q)}{(1 - \nu)\sqrt{p^2 - 4q}} \right) \right]_0^{\nu_0}. \tag{A6}$$

When $n_2^\Sigma = 0$ and $n_{-2}^\Sigma > 0$, the first formula is no longer valid but can be replaced with:

$$g_1 = \frac{S_A}{\mathcal{F}} \sqrt{\frac{\kappa_s}{\mathcal{I}}} \frac{1}{p} (\sqrt{1 - p\nu_0} - 1). \tag{A7}$$

Similarly, Eq. (A6) is not valid when $n_{-2}^\Sigma = 0$ and $n_2^\Sigma > 0$, but can then be replaced with:

$$g_{-1} = \frac{S_A}{\mathcal{F}} \sqrt{\frac{\kappa_s}{\mathcal{I}}} \left[\frac{\sqrt{q(\nu^2 - 1) + p(1 - \nu)}}{2 q(\nu - 1) + p(1 - \nu)} \right]_0^{\nu_0} \tag{A8}$$

To calculate surface excesses of divalent ions, [12] pointed out that we can reuse the values found for the monovalent ions. First, the Grahame equation can be rewritten as:

$$\sigma = \frac{\nu_0}{1 - \nu_0} \cdot \sqrt{\kappa_s \mathcal{I}} \cdot \sqrt{q\nu_0^2 - p\nu_0 + 1}. \tag{A9}$$

After inserting $n_{-1}^\Sigma \equiv n_1^\Sigma + 2(n_2^\Sigma - n_{-2}^\Sigma)$ (charge balance) into this equation, and further making use of Eqs. (24), (A2),

and (A3) to express $n^{\Sigma}_{-2} = (q - p + 1)\mathcal{I}$, we end up with:

$$g_2 = \frac{\frac{S_A}{\mathcal{F}}\left(\frac{\sigma(1-v_0)}{v_0} - \sqrt{\kappa_s\mathcal{I}}\right) - n^{\Sigma}_1 g_1}{2n^{\Sigma}_2} . \qquad (A10)$$

$$g_{-2} = \frac{\frac{S_A}{\mathcal{F}}\left(\frac{\sigma}{v_0} - \sqrt{\kappa_s\mathcal{I}}\right) - n^{\Sigma}_{-1} g_{-1}}{2n^{\Sigma}_{-2}} . \qquad (A11)$$

1:2-electrolyte

For a 1:2-electrolyte (e.g., Na_2SO_4), we have

$$\mathcal{I} = \frac{3}{2} \cdot n^{\Sigma}_1 . \qquad (A12)$$

$$p = \frac{2}{3} . \qquad (A13)$$

Thus, Eq. (A7) reduces to

$$g_1 = \frac{S_A}{\mathcal{F}} \sqrt{\frac{\kappa_s}{\mathcal{I}}} \cdot \sqrt{\frac{3}{2}}\left[\sqrt{\frac{3}{2} - v_0} - \sqrt{\frac{3}{2}}\right] . \qquad (A14)$$

Similarly, Eqs. (A9) and (A11) together yield:

$$g_{-2} = \frac{S_A}{\mathcal{F}} \sqrt{\frac{\kappa_s}{\mathcal{I}}} \cdot \sqrt{\frac{3}{2}}\left[\frac{\sqrt{\frac{3}{2} - v_0}}{1 - v_0} - \sqrt{\frac{3}{2}}\right] . \qquad (A15)$$

The above two equations follow directly from equations (35) and (36) in [4].

2:1-electrolyte

For a 2:1-electrolyte (e.g., $CaCl_2$ or $MgCl_2$), we have

$$\mathcal{I} = 3 \cdot n^{\Sigma}_2 . \qquad (A16)$$

$$p = \frac{4}{3} . \qquad (A17)$$

$$q = \frac{1}{3} . \qquad (A18)$$

Combining Eqs. (A9) and (A10) leads to:

$$g_2 = \frac{S_A}{\mathcal{F}} \sqrt{\frac{\kappa_s}{\mathcal{I}}} \frac{3}{2} \left(\frac{1}{\sqrt{3}}\sqrt{(3 - v_0)(1 - v_0)} - 1\right) \qquad (A19)$$

After some algebra, Eq. (A8) reduces to

$$g_{-1} = \frac{S_A}{\mathcal{F}} \sqrt{\frac{\kappa_s}{\mathcal{I}}} \frac{3}{2} \left(\frac{1}{\sqrt{3}}\sqrt{\frac{3 - v_0}{1 - v_0}} - 1\right) . \qquad (A20)$$

These two equations could also be derived from equations (45) and (46) in [4].

Appendix B Tables

Table 1 Table of computed log K values for surface- and aqueous complexes in the carbonate SCM

Complex (secondary specie)	Basis species	logK @ 25°C
$CaOH^+$	$\rightleftharpoons Ca^{2+} + H_2O - H^+$	12.83
$CO_2(aq)$	$\rightleftharpoons H^+ + HCO_3^- - H_2O$	-6.34
CO_3^{2-}	$\rightleftharpoons HCO_3^- - H^+$	10.33
$CaCO_3^0$	$\rightleftharpoons Ca^{2+} + HCO_3^- - H^+$	7.00
$CaHCO_3^+$	$\rightleftharpoons Ca^{2+} + HCO_3^-$	-1.05
$CaSO_4^0$	$\rightleftharpoons Ca^{2+} + SO_4^{2-}$	-2.11
HSO_4^-	$\rightleftharpoons H^+ + SO_4^{2-}$	-1.98
$NaOH^0$	$\rightleftharpoons Na^+ + H_2O - H^+$	14.20
OH^-	$\rightleftharpoons H_2O - H^+$	14.00
$NaSO_4^-$	$\rightleftharpoons Na^+ + SO_4^{2-}$	-0.70
$>CaSO_4^-$	$\rightleftharpoons >CaH_2O^+ + SO_4^{2-}$	-2.11
$>CaCO_3^-$	$\rightleftharpoons >CaH_2O^+ + HCO_3^- - H^+$	7.00
$>CaOH^0$	$\rightleftharpoons >CaH_2O^+ + H_2O - H^+$	12.83
$>CaHCO_3^0$	$\rightleftharpoons >CaH_2O^+ + H_2O$	-1.05
$>CO_3H^0$	$\rightleftharpoons >CO_3^- + H^+$	-4.88
$>CO_3Ca^+$	$\rightleftharpoons >CO_3^- + Ca^{2+}$	-1.74
$>CO_3Mg^+$	$\rightleftharpoons >CO_3^- + Mg^{2+}$	-1.04
calcite	$\rightleftharpoons Ca^{2+} + HCO_3^- - H^+$	1.85
$CO_2(g)$	$\rightleftharpoons HCO_3^- + H^+ - H_2O$	-7.81

Table 2 Solution chemistry for seawater in equilibrium with calcite without calculation of surface excess ($f_{DL} = 1$) ($S_A = 3000.0 \, m^2/L$), pH= 7.4, $\sigma = -0.00125$ C/m^2, $\psi_0 = -0.705$ mV

Basis specie	n_i^{tot}	n_i^{aq}	$n_i^{surface}$
Ca^{2+}	1.30E-02	1.29E-02	3.06E-03
Cl^-	5.25E-01	5.25E-01	0.00E+00
H^+	7.39E-05	6.09E-05	1.30E-05
H_2O	1.00E+00	1.00E+00	6.85E-08
HCO_3^-	2.00E-03	1.94E-03	2.55E-04
K^+	1.00E-02	1.00E-02	0.00E+00
Mg^{2+}	4.45E-02	4.45E-02	2.43E-03
Na^+	4.50E-01	4.50E-01	0.00E+00
SO_4^{2-}	2.40E-02	2.40E-02	5.39E-03
$>CO_3^-$	2.47E-02	0.00E+00	2.47E-02
$>CaH_2O^+$	2.47E-02	0.00E+00	2.47E-02
E_0	9.73E-01	0	9.73E-01

Table 3 Solution chemistry for a 0.024 M Na_2SO_4 solution in equilibrium with calcite and CO_2 when using the full diffuse layer model including surface excess. The partial pressure of CO_2 was set to $P_{CO_2} = 10^{-3.4}$, and the size of the diffuse layer was 10.0 nm, which gave $f_{DL} = 0.03$ ($S_A = 3000.0$ m^2/L). pH= 8.6, $\sigma = -0.020$ C/m^2, $\psi_0 = -35.0$ mV

Basis specie	n_i^{tot}	n_i^{aq}	$n_i^{surface}$	n_i^{Γ}	$n_{DL,i}$
H^+	-2.21e-4	-1.02e-04	-1.17e-04	6.30e-07	-2.44e-06
Ca^{+2}	1.79e-3	2.65e-04	1.51e-03	4.27e-06	1.22e-05
HCO_3^-	3.43e-3	3.07e-03	2.88e-04	-1.16e-05	8.06e-05
Na^+	4.80e-02	4.77e-02	0	3.35e-04	1.76e-03
SO_4^{-2}	2.40e-02	2.25e-02	1.62e-03	-1.28e-04	5.47e-04
$>CaH_2O^+$	2.47e-02	0	2.47e-02	0	0
$>CO_3^-$	2.47e-02	0	2.47e-02	0	0
E_0	2.56e-01	0	2.56e-01	0	0

Table 4 Solution chemistry for a 0.024 M brine in equilibrium with calcite and CO_2 ($P_{CO_2} = 10^{-3.4}$), when using the proposed ion exchange model with log $K = 0$ for all ion exchange half-reactions: The size of the diffuse layer was set to 10.0 nm, which gave $f_{DL} = 0.03$ ($S_A = 3000.0$ m^2/L). pH= 8.6, $\sigma = -0.019$ C/m^2, $\psi_0 = -35.0$ mV

Basis specie	n_i^{tot}	n_i^{aq}	$n_i^{surface}$	$n_{DL,i}$
H^+	-2.23e-4	-1.03e-04	-1.20e-04	1.27e-10
Ca^{+2}	1.82e-3	2.57e-04	1.49e-03	7.30e-05
HCO_3^-	3.41e-3	3.09e-03	2.92e-04	2.91e-05
Na^+	4.80e-02	4.61e-02	0	1.85e-03
SO_4^{-2}	2.40e-02	2.17e-02	1.58e-03	6.84e-04
$>CaH_2O^+$	2.47e-02	0	2.47e-02	0
$>CO_3^-$	2.47e-02	0	2.47e-02	0
E_0	2.56e-01	0	2.56e-01	0
YDL^-	2.00e-03	0	0	2.00e-03
YDL^+	1.40e-03	0	0	1.40e-03

Table 5 Ion exchange model for the diffuse layer: log K values used in four example cases

Ion exchange half-reaction	Case 1	Case 2	Case 3	Case 4
$Na - Y_{DL} \rightleftharpoons Na^+ + Y_{DL}^-$	0	0	-6	0
$H - Y_{DL} \rightleftharpoons H^+ + Y_{DL}^-$	0	-7	0	0
$Ca - Y_{DL2} \rightleftharpoons Ca^{2+} + 2Y_{DL}^-$	0	-0.8	0	-6
$HCO_3 - Y_{DL} \rightleftharpoons HCO_3^- + Y_{DL}^+$	0	-2	-6	0
$SO_4 - Y_{DL2} \rightleftharpoons SO_4^{2-} + 2Y_{DL}^+$	0	0	0	-6

Table 6 Total concentrations in the diffuse layer when using the full diffuse layer model including surface excess and the exchange model; log K values are listed in Table 5. Note that in the EDL approach, secondary complexes like $NaSO_4^-$ are included in the total. For the exchange model, only free ions can adsorb

	$TOTNa^+$	$TOTH^+$	$TOTCa^{+2}$	$TOTHCO_3^-$	$TOTSO_4^{-2}$
EDL	1.76e-03	-2.44e-06	1.22e-05	8.06e-05	5.47e-04
Case 1	1.85e-03	1.27e-10	7.30e-05	2.91e-05	6.84e-04
Case 2	1.02e-03	7.15e-04	1.44e-04	1.18e-03	1.21e-04
Case 3	1.96e-03	1.64e-16	1.24e-16	1.40e-03	2.36e-12
Case 4	9.74e-06	4.96e-13	1.05e-03	3.92e-08	7.22e-04

Declarations

Competing interests None.

References

1. Gouy, M.: Sur la constitution de la charge électrique á la surface d'un électrolyte. J. Phys. Theor. Appl. **9**(1), 457–468 (1910). https://doi.org/10.1051/jphystap:019100090045700

2. Chapman, D.L.: A contribution to the theory of electrocapillarity. The London, Edinburgh, and Dublin Philosophical Magazine and Journal of Science **25**(148), 475–481 (1913). https://doi.org/10.1080/14786440408634187

3. Grahame, D.C.: The electrical double layer and the theory of electrocapillarity. Chemical Reviews **41**(3), 441–501 (1947). https://doi.org/10.1021/cr60130a002

4. Grahame, D.C.: Diffuse double layer theory for electrolytes of unsymmetrical valence types. The J Chem Phys **21**(6), 1054–1060 (1953). https://doi.org/10.1063/1.1699109

5. Israelachvili, J.N.: Intermolecular and Surface Forces, 3rd edn. (2011)

6. Appelo, C.A.J., Postma, D.: Geochemistry, Groundwater and Pollution, 2nd edn. A.A. Balkema Publishers, Leiden (2005)

7. Lützenkirchen, J., Marsac, R., Kulik, D.A., Payne, T.E., Xue, Z., Orsetti, S., Haderlein, S.B.: Treatment of multi-dentate surface complexes and diffuse layer implementation in various speciation codes. Applied Geochemistry **55**, 128–137 (2015). https://doi.org/10.1016/j.apgeochem.2014.07.006

8. unter, R.J.: Zeta Potential in Colloid Science: Principles and Applications. Academic Press, London (2013)

9. Borkovec, M., Westall, J.: Solution of the Poisson-Boltzmann equation for surface excesses of ions in the diffuse layer at the oxide-electrolyte interface. J Electroanal Chem Interfacial Electrochem **150**(1–2), 325–337 (1983). https://doi.org/10.1016/S0022-0728(83)80214-9

10. Lohne, A., Nødland, O., Stavland, A., Hiorth, A.: A model for non-newtonian flow in porous media at different flow regimes. Comput

Geosci **21**(5), 1289–1312 (2017). https://doi.org/10.1007/s10596-017-9692-6

11. Lohne, A.: User's Manual for IORCoreSim - Combined EOR and SCAL Simulator. Norwegian Research Centre (NORCE), (2022). Norwegian Research Centre (NORCE)

12. Oldham, K.B.: Composition of the diffuse double layer in seawater or other media containing ionic species of +2, +1, -1, and -2 charge types. J Electroanal Chem Interfacial Electrochem **63**(2), 139–156 (1975). https://doi.org/10.1016/S0022-0728(75)80287-7

13. Garrels, R.M., Christ, C.L.: Solutions, Minerals, and Equilibria. Harper and Row, New York (1965)

14. Bethke, C.M.: Geochemical and Biogeochemical Reaction Modeling, 3rd edn. Cambridge University Press, Cambridge, UK (2022)

15. Helgeson, H.C., Kirkham, D.H.: Theoretical prediction of the thermodynamic behavior of aqueous electrolytes at high pressures and temperatures; I, Summary of the thermo dynamic/electrostatic properties of the solvent. American J Sci **274**(10), 1089–1198 (1974). https://doi.org/10.2475/ajs.274.10.1089

16. Helgeson, H.C., Kirkham, D.H.: Theoretical prediction of the thermodynamic behavior of aqueous electrolytes at high pressures and temperatures; II, Debye-Huckel parameters for activity coefficients and relative partial molal properties. American J Sci **274**(10), 1199–1261 (1974). https://doi.org/10.2475/ajs.274.10.1199

17. Johnson, J.W., Oelkers, E.H., Helgeson, H.C.: Supcrt92: A software package for calculating the standard molal thermodynamic properties of minerals, gases, aqueous species, and reactions from 1 to 5000 bar and 0 to 1000 c. Computers & Geosciences **18**(7), 899–947 (1992). https://doi.org/10.1016/0098-3004(92)90029-Q

18. Van Cappellen, P., Charlet, L., Stumm, W., Wersin, P.: A surface complexation model of the carbonate mineral-aqueous solution interface. Geochimica et Cosmochimica Acta **57**(15), 3505–3518 (1993). https://doi.org/10.1016/0016-7037(93)90135-J

19. Hiorth, A., Cathles, L., Madland, M.: The impact of pore water chemistry on carbonate surface charge and oil wettability. Transport In Porous Media **85**(1), 1–21 (2010). https://doi.org/10.1007/s11242-010-9543-6

20. Stumm, W.: Chemistry of the Solid-Water Interface. Wiley-Interscience, New York (1992)

21. Kontogeorgis, G.M., Maribo-Mogensen, B., Thomsen, K.: The Debye-Hückel theory and its importance in modeling electrolyte solutions. Fluid Phase Equilibria **462**, 130–152 (2018). https://doi.org/10.1016/j.fluid.2018.01.004

22. Heberling, F., Trainor, T.P., Lützenkirchen, J., Eng, P., Denecke, M.A., Bosbach, D.: Structure and reactivity of the calcite-water interface. Journal of Colloid and Interface Science **354**(2), 843–857 (2011). https://doi.org/10.1016/j.jcis.2010.10.047

23. Thompson, D.W., Pownall, P.G.: Surface electrical properties of calcite. Journal of Colloid and Interface Science **131**(1), 74–82 (1989). https://doi.org/10.1016/0021-9797(89)90147-1

24. Parkhurst, D.L., Appelo, C.A.J.: User's Guide PHREEQC (Version 2) a Computer Program for Speciation. One-Dimensional Transport, and Inverse Geochemical Calculations, Batch-Reaction (1999)

25. Sherman, D.: Surface complexation modeling: Mineral fluid equilibria at the molecular scale. Thermodynamics and Kinetics of Water-Rock Interaction, 181–206 (2009). https://doi.org/10.2138/rmg.2009.70.5

26. Bonto, M.: Numerical modelling and upscaling of modified salinity waterflooding. PhD thesis, Danish Hydrocarbond Research and Technology Centre, Technical University of Denmark (DTU) (2021)

27. Al Mahrouqi, D., Vinogradov, J., Jackson, M.D.: Zeta potential of artificial and natural calcite in aqueous solution. Advances in Colloid and Interface Science **240**, 60–76 (2017). https://doi.org/10.1016/j.cis.2016.12.006

28. Mahani, H., Keya, A.L., Berg, S., Nasralla, R.: Electrokinetics of carbonate/brine interface in low-salinity waterflooding: Effect of brine salinity, composition, rock type, and ph on ζ-potential and a surface-complexation model. SPE Journal **22**(01), 53–68 (2017). https://doi.org/10.2118/181745-PA

29. Maghsoudian, A., Esfandiarian, A., Kord, S., Tamsilian, Y., Soulgani, B.S.: Direct insights into the micro and macro scale mechanisms of symbiotic effect of SO2- 4, Mg2+, and Ca2+ ions concentration for smart water flooding in the carbonated coated micro model system. J Mol Liq **315**, 113700 (2020). https://doi.org/10.1016/j.molliq.2020.113700

30. Megawati, M., Hiorth, A., Madland, M.: The Impact of Surface Charge on the Mechanical Behavior of High-Porosity Chalk. Rock Mechanics and Rock Engineering **46**(5), 1073–1090 (2013). https://doi.org/10.1007/s00603-012-0317-z

31. Minde, M.W., Hiorth, A.: Compaction and fluid–rock interaction in chalk insight from modelling and data at pore-, core-, and field scale. Geosciences **10**(1) (2020). https://doi.org/10.3390/geosciences10010006

32. Megawati, Hiorth, A., Madland, M.V.: The effect of sulfate adsorption on the cation exchange capacity of high porosity chalks. Goldschmidt conference Prague, Geochemical Society and the European Association of Geochemistry (2011)

33. Jenny, H.: Studies on the Mechanism of Ionic Exchange in Colloidal Aluminum Silicates. The J Phys Chem **36**(8), 2217–2258 (1932). https://doi.org/10.1021/j150338a011

34. Marcus, Y.: Ionic radii in aqueous solutions. Chemical Reviews **88**(8), 1475–1498 (1988). https://doi.org/10.1021/cr00090a003

35. Bruggenwert, M., Kamphorst, A.: Survey of experimental information on cation exchange in soil systems. In: Developments in Soil Science vol. 5, pp. 141–203. Elsevier, London (1979). https://doi.org/10.1016/S0166-2481(08)70660-3

36. Kleven, R., Alstad, J.: Interaction of alkali, alkaline-earth and sulphate ions with clay minerals and sedimentary rocks. J Petrol Sci Eng **15**(2–4), 181–200 (1996). https://doi.org/10.1016/0920-4105(95)00085-2

37. Brouwer, E., Baeyens, B., Maes, A., Cremers, A.: Cesium and rubidium ion equilibriums in illite clay. The J Phys Chem **87**(7), 1213–1219 (1983). https://doi.org/10.1021/j100230a024

38. Maes, A., Cremers, A.: Highly Selective Ion Exchange in Clay Minerals and Zeolites. In: Davis, J.A., Hayes, K.F. (eds.) Geochemical Processes at Mineral Surfaces, pp. 254–295. American Chemical Society, Washington, DC (1986). https://doi.org/10.1021/bk-1987-0323.ch013

39. Shainberg, I., Kemper, W.: Hydration Status of Adsorbed Cations. Soil Sci Soc Am J **30**(6), 707–713 (1966). https://doi.org/10.2136/sssaj1966.03615995003000060017x

40. Teppen, B.J., Miller, D.M.: Hydration Energy Determines Isovalent Cation Exchange Selectivity by Clay Minerals. Soil Sci Soc Am J **70**(1), 31–40 (2006). https://doi.org/10.2136/sssaj2004.0212

41. Appelo, C.A.J., Parkhurst, D.L.: Calculating cation exchange with PHREEQC (version 2) (2002)

42. Gaines Jr, G.L., Thomas, H.C.: Adsorption Studies on Clay Minerals. II. A formulation of the Thermodynamics of Exchange Adsorption. The J Chem Phys **21**(4), 714–718 (1953). https://doi.org/10.1063/1.1698996